

# Effect of Inflow on Computational Fluid Dynamic Simulation of Cerebral Bifurcation Aneurysms

A. Farnoush, Y. Qian, A. Avolio

**Abstract**— Morphological characteristics associated with cerebral aneurysm formation can be used to assess aneurysm rupture. This study investigated hemodynamic effects resulting from change in the parent artery diameter of bifurcation type aneurysm. Computational fluid dynamic (CFD) analysis was performed on middle cerebral artery (MCA) models with various parent artery diameters. Calculations were performed with steady flow rate ( $125 \pm 12.5$  ml/min) at the parent artery inlet. Energy loss (EL) was calculated from pressure and kinetic energy obtained from flow velocity. The results indicate that the high wall shear stress (WSS) and EL occurs in model with the smallest parent vessel compared to the other models for all three inflows. Results also showed that 10% variation of inflow results in average of  $23 \pm 2.9\%$  changes in WSS and  $25.5 \pm 0.5\%$  changes in energy loss. These results demonstrated that for CFD analysis of MCA bifurcation type aneurysm, upstream parent vessel and inflow evaluation for individual patient is essential.

## I. INTRODUCTION

The prevalence of unruptured intracranial aneurysms is reported to be between 2% [1] and 5% [2]. Investigations of the relationship between aneurysm location and its rupture indicated that the anterior communicating artery and the middle cerebral artery, where aneurysms are located at the bifurcation, bleeds easily in contrast with lateral aneurysms such as those found at the branching and bending points on the internal carotid artery [3]. The rank order of decreasing aneurysm size for ruptured lesions has been found to be ophthalmic, internal carotid artery (ICA) bifurcation, basilar bifurcation, middle cerebral artery (MCA) bifurcation, posterior communicating artery (Pcomm), anterior communicating artery (Acomm), posterior inferior cerebellar artery (PICA), and distal aneurysms.[4]

However the relationship between these parameters in aiding neurosurgeons to choose the best preventive treatment for unruptured aneurysm and considering the risk of surgical outcome are still unknown, despite the study of 263 patients

Manuscript received March 20, 2011. The study is supported by a Macquarie University Research Excellence Scholarship (MQRES).

A.Farnoush is with the Australia School of Advanced Medicine, Macquarie University (email: azadeh.farnoush@students.mq.edu.au)

Y. Qian is with the Australia School of Advanced Medicine, Macquarie University, Sydney, Australia (email: yi.qian@mq.edu.au)

A.Avolio is with the Australia School of Advanced Medicine, Macquarie University, Sydney, Australia (email: alberto.avolio@mq.edu.au)

with 339 MCA aneurysms showing that age and aneurysm size are the only 2 independent predictors of surgical outcome. [5]

On the other hand, calculated energy loss (EL) in ruptured and unruptured aneurysms at the internal carotid artery (ICA) based on patient-specific computational fluid dynamics (CFD) models showed a significant difference between EL in ruptured and unruptured aneurysms (average values of 167 Pa, 6.3 Pa respectively) suggesting that the magnitude of EL may have an effect on aneurysm rupture [6].

Our hypothesis is that the formation of the aneurysm at the apex of the bifurcation leads to change in energy balance of the vasculature associated with the aneurysm. Therefore investigating changes in energy balance due to morphological variation could explain the risk of rupture. The purpose of this study was to elucidate the poorly understood hemodynamic effects resulting from different geometry and sizes of the parent vessels of cerebral aneurysm. The first step was to clarify the relationship between hemodynamic forces and parent artery diameters in an attempt to establish clear correlations to evaluate risk of rupture and improve the management of unruptured aneurysms.

## II. METHODOLOGY

### A. Idealized bifurcation model

CFD analysis of patient specific models due to a variety of parameters such as geometry, location of the aneurysm and different morphology of parent vessels have limitations that can affect calculated hemodynamic parameters. Therefore an idealized three dimensional model was built of MCA bifurcation aneurysms using ANSYS Workbench 12.1 to increase the performance of patient specific modeling. The basic aneurysm (Model A) was designed to have a 3.5 mm height (H), 5.2 mm sac diameter (D) with neck width (N) of 4.0 mm. A straight parent artery of diameter (Dp) 2.0 mm was connected to two branches of 2.0 mm diameter (Db), as shown in Fig. 1a [7]. Model B and C were modified to have a similar aneurysm configuration and branch diameters with parent artery diameter of 3.0 mm and 4.0 mm. Bifurcation angle was set at  $180^\circ$  in all models.

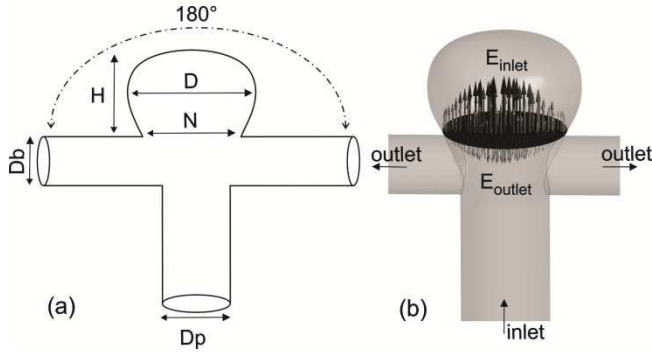


Fig. 1. (a) Symmetric bifurcation aneurysm at MCA. Bifurcation angle was  $180^\circ$ . 2.0 mm parent artery ( $D_p$ ) and 2.0 mm branch arteries ( $D_b$ ) were selected for the idealized model. Sac diameters ( $D$ ) of the aneurysms were set at 5.2 mm. (b)  $E_{inlet}$  and  $E_{outlet}$  are the spatially averaged energy values over the cross section of the neck.

**TABLE I:** CALCULATED ENERGY LOSS USING (1) AND (2) AT DIFFERENT INFLOWS AND FLOW DIVISIONS. ALL DIMENSIONS ARE IN PASCAL (PA).

$D_p$ (mm)	Inflow at 60:40 flow division			Flow division at branches for value 125 (ml/min)		
	112.5*	125*	137.5*	60:40	70:30	80:20
2	116.8	152.1	185.1	152.1	86.8	75.0
3	42.5	53.3	65.3	53.3	53.0	50.3
4	10.6	13.6	17.0	13.6	13.2	12.3

\* Inflow dimensions are in (ml/min).

### B. Computational Analysis

To characterize the flow regime in the parent artery and branches, an incompressible, steady-state laminar flow model was considered for the simulation. In the large arteries (diameter  $> 0.5$  mm) or for very low shear rates, the Non-Newtonian behavior of blood flow is negligible. Therefore, blood was assumed to be a Newtonian fluid [8], [9] with density and dynamic viscosity of  $1050 \text{ kg/m}^3$  and  $0.0035 \text{ Pa}\cdot\text{s}$  respectively [10]. Arteries were assumed to be rigid where a no-slip boundary condition was imposed. Three flow distributions of 60:40, 70:30 and 80:20 were prescribed at extended outlets to cover all the possibility of flow division between two branches of three dimensional idealized models. Investigating the stability of pulsatile blood flow at the neck of cerebral aneurysm (sidewall and bifurcation) showed that analysis of steady, non-pulsatile flow in many cases can provide reasonable information about intra-aneurysmal flow in addition to be faster and time-dependant [11]. Therefore calculations were performed with steady flow rate ( $125 \pm 12.5 \text{ ml/min}$ ) at the parent artery inlet.

The commercial finite volume software (ANSYS® CFX.12.1) was used to analyze the flow model and CFD simulations.

The energy loss dissipated for a blood flow transition through the bifurcation for a specific control volume of each idealized model satisfies:

$$\text{Energy loss (EL)} = E_{inlet} - E_{outlet} \quad (1)$$

$$EL_{Aneurysm} = \underbrace{\sum \left( P_i + \rho \frac{1}{2} v_i^2 \right)}_{E_{inlet}} - \underbrace{\sum \left( P_o + \rho \frac{1}{2} v_o^2 \right)}_{E_{outlet}} \quad (2)$$

where  $\rho$ ,  $P$  and  $v$  are the fluid density, static pressure and velocity respectively;  $i$  indicates the inflow to the aneurysm;  $o$  the outflow of aneurysm (Fig. 1b).  $E_{inlet}$  and  $E_{outlet}$  are the spatially averaged energy values over the cross section of the neck.

## III. RESULTS

### A. Effect of inflow on energy loss

Accuracy of the numerical simulation can be affected by imprecise upstream parent artery evaluation [12]. In addition, an irregular shape of the parent artery in patient specific models with various diameters at different locations can affect the velocity of the jet flow at the apex of the bifurcation. Hence, to analyze the intra-aneurysmal flow, calculation of flow velocity at the proximal part of the bifurcation is necessary.

To examine this phenomenon for a range of inflow of  $125 \pm 12.5 \text{ ml/min}$ , the energy loss of the aneurysm neck was calculated using (1) (Table I).

The results indicate that for all models increasing the inflow leads to augmentation of kinetic energy, term

$< \rho \frac{1}{2} v^2 >$ , and energy loss.

Comparison of the results showed that as inflow increases from  $112.5 \text{ ml/min}$  to  $125 \text{ ml/min}$  and then from  $125 \text{ ml/min}$  to  $137.5 \text{ ml/min}$ , the energy loss increases with average of  $27 \pm 2.5\%$  and  $23 \pm 1.8\%$  respectively. A  $D_p$  of 2.0 mm is more sensitive to inflow changes due to augmentation of velocity in smaller vessel diameter for specific nominal inflow.

### B. Effect of flow distribution at the branches of bifurcation

Distribution of blood flow in the bifurcation branches in a patient specific model is poorly understood and cannot be readily measured non-invasively. Therefore to increase the accuracy of estimation for a nominal value of  $125 \text{ ml/min}$  inflow, different flow distributions were examined for all models.

As shown in Table I, energy loss of model A with a 2.0 mm parent vessel is more sensitive to distribution of flow at branches. The average of energy losses for all three flow divisions were calculated  $104.6 \pm 41 \text{ Pa}$ ,  $52 \pm 1.7 \text{ Pa}$ ,  $13 \pm 0.6 \text{ Pa}$  for model A, B and C respectively.

### C. Energy loss with respect to parent artery diameter

Comparison of the flow pattern inside the aneurysm at a center section of all three models showed that the flow is asymmetric with inflow near the dominant branch and outflow near the branch with smaller flow (Fig. 2a). The location of a vortex center varied with parent vessel diameter, approaching close to the neck for models with the larger parent diameter (model B and C) and close to the dome for model A with the smallest parent vessel.

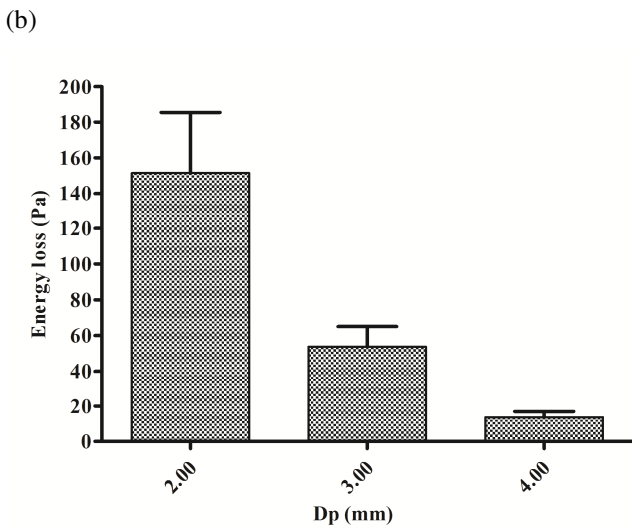
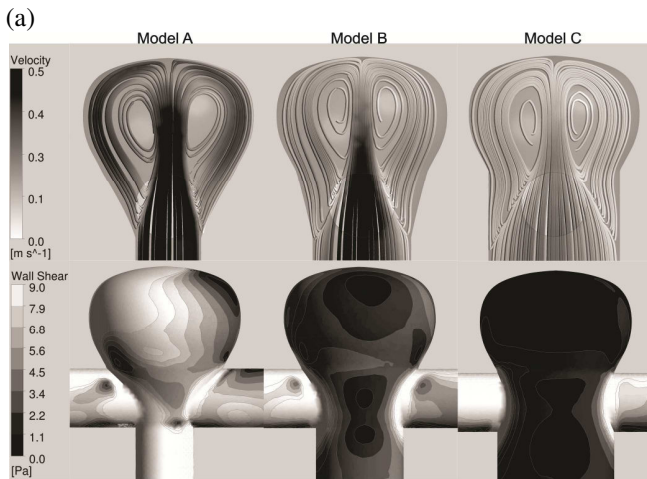


Fig. 2. (a) Application of CFD to MCA bifurcation aneurysm .The only single changing parameter among the three models was the parent artery diameter; *Top row*: Typical velocity streamlines (m per second) demonstrating the difference in intra-aneurysmal flow between models *bottom row*: Typical Wall shear stress maps (Pa) revealing the highest shear stress area in model A and the lowest in model C. (b) EL calculated at aneurysm neck as a function of parent vessel diameter (Dp). The flow distribution of 60:40 was selected as it had the greatest effect on energy loss. Error bars indicate standard deviation of EL values determined for the three inflows of 112.5 ml/min, 125 ml/min and 137.5 ml/min.

Fig. 2b suggests that the aneurysm in model A loses the highest energy for a range of inflow (125 ml/min  $\pm$  12.5) compared to model B and C (model A: 151  $\pm$  34; Model B: 53  $\pm$  11; model C: 13  $\pm$  3 for flow division of 60:40)

#### D. Wall shear stress with respect to parent artery diameter

Wall shear stress (WSS) is defined as the tangential force per unit area that is exerted by the moving fluid on the surface of the artery and its magnitude is proportional to the velocity gradient near the artery surface [13].

For bifurcations studied with parent vessels of different diameters, the average WSS on the aneurysm surface is shown in Fig.2a and Fig. 3. Generally, the results show that by increasing the inflow, WSS increases, whereas the highest WSS occurs in model A compared to model B and C

(as flow increases from 112.5 ml/min to 125 ml/min and from 125ml/min to 137.5 ml/min, the WSS increases with average of 25  $\pm$  3.7% and 21  $\pm$  1.2% respectively)

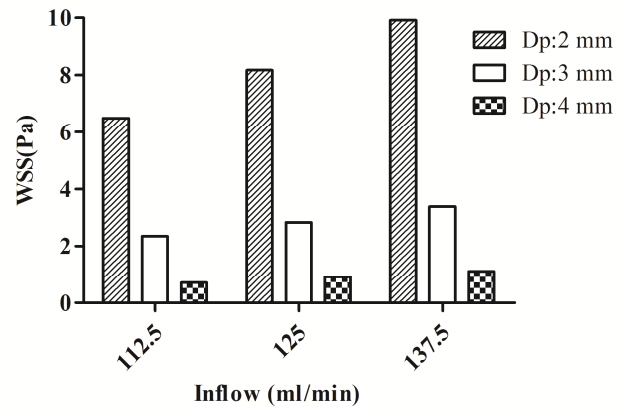


Fig. 3. WSS calculated at aneurysm surface for different parent artery diameter (Dp) as a function of inflow for 60:40 flow distribution.

#### IV. DISCUSSION

Morphological characteristics of aneurysms and their effect on initiation, growth and rupture of aneurysm have been extensively studied suggesting that aneurysm size and shape irregularity are two independent factors predicting rupture [14],[15]. But the roles of the parent vessel geometries which provide the jet flow at the apex of the bifurcation are poorly understood. Our results showed that for similar aneurysm and inflow, parent vessel size can change the energy loss from 10.6 Pa to 116.8 Pa for 4.0 mm and 2.0 mm parent artery diameters respectively. Therefore considering the morphological characteristic of the aneurysm by itself cannot provide enough information for making decisions about the treatment.

Castro, in 2006, showed that CFD modeling of truncated parent vessels underestimated the magnitude of WSS and corresponding hemodynamic parameters [12]. These findings are in good agreement with our results suggesting that modeling bifurcation aneurysms without considering the geometry of the parent artery can underestimate hemodynamic parameters such as energy loss and WSS.

Due to noise and insufficient resolution, phase contrast magnetic resonance imaging (PC MRI) may not have precise geometry and velocity information, which can affect the quality of the numerical simulation [16]. In this present study, by assuming 10% deviation for assumed inflow, we explore the importance of upstream parent artery evaluation.

Evaluation of flow distribution at branches of a bifurcation is poorly understood. The assumption of a zero pressure boundary condition in CFD modeling of patient specific model causes the flow rates in the outflow segments to be determined according to their resistances, whereas in reality this is determined not only by the resistance of those segments but also by the resistance of all distal vessels. Thus, the sensitivity of the patient-specific results to flow splits in the outflow segments also needs to be addressed. Our results suggest that until there is access to non-invasive

measurement of flow at branches, various distributions should be considered for numerical simulations.

For MCA aneurysms, Cebal *et al* suggested two types of flow patterns in MCA aneurysms: type III (43%) (changing direction of inflow jet with creation of a single vortex) and type I (29%) (unchanging direction of inflow jet with a single associated vortex) [17]. Our results showed that type III flow can be seen inside the aneurysm.

The study of magnitude of WSS in 20 MCA aneurysm conducted by Shojima *et al* suggests the pathogenic effect of a high WSS in the initiating the aneurysm. A low WSS may facilitate the growth and may trigger the rupture of a cerebral aneurysm [18]. These results were obtained by considering the same velocity profile at inlet condition for all patient specific models. However, our results showed that the high WSS and energy loss occurs in model A with the smallest parent vessel compared to the other models if the inflow coming from the internal carotid artery (ICA) was the same. This study agrees with previous work showing that, the possibility of different inflow for each patient needs to be accounted for CFD analysis of patient-specific models [19].

Compliant models of cerebral aneurysms were not used in the present study for two main reasons: I) its high demand in terms of computational time, II) the necessity to validate the required information (aneurysmal wall compliance) which is not within the scope of this study. However, the presented results are useful in establishing more accurate numerical simulation of cerebral aneurysms and can be used in clinical trials.

## V. CONCLUSION

Based on data presented in this study, evaluation of flow in upstream parent vessel and flow division at branches is essential. Our results indicates that even 10% variation of inflow results in average of  $23 \pm 2.9\%$  changes in WSS and  $25.5 \pm 0.5\%$  changes in energy loss that could affect any conclusion from the hemodynamic results of MCA bifurcation type aneurysm modeling. .

## REFERENCES

- [1] G. Rinkel, M. Djibuti, A. Algra, and J.V. Gijn, "Prevalence and risk of rupture of intracranial aneurysms: a systematic review," *Stroke*, vol. 29, 1998, pp. 251-256.
- [2] H.R. Winn, J. a Jane, J. Taylor, D. Kaiser, and G.W. Britz, "Prevalence of asymptomatic incidental aneurysms: review of 4568 arteriograms," *Journal of neurosurgery*, vol. 96, Jan. 2002, pp. 43-9.
- [3] H. Ujiie, K. Sato, H. Onda, a Oikawa, M. Kagawa, K. Takakura, and N. Kobayashi, "Clinical analysis of incidentally discovered unruptured aneurysms.," *Stroke; a journal of cerebral circulation*, vol. 24, Dec. 1993, pp. 1850-6.
- [4] B.S. Carter, S. Sheth, E. Chang, M. Sethl, and C.S. Ogilvy, "Epidemiology of the size distribution of intracranial bifurcation aneurysms: smaller size of distal aneurysms and increasing size of unruptured aneurysms with age," *Neurosurgery*, vol. 58, 2006, p. 217.
- [5] M.K. Morgan, W. Mahattanakul, A. Davidson, and J. Reid, "Outcome for middle cerebral artery aneurysm surgery.," *Neurosurgery*, vol. 67, Sep. 2010, pp. 755-61; discussion 761.
- [6] Y. Qian, T. Harada, K. Fukui, M. Umezu, H. Takao, and Y. Murayama, "Hemodynamic Analysis of Cerebral Aneurysm and

- Stenosed Carotid Bifurcation Using Computational Fluid Dynamics Technique," *Lecture Notes in Computer Science*, vol. 4689/2007, 2007, pp. 292-299.
- [7] F. Umansky, S.M. Juarez, M. Dujovny, J.I. Ausman, F.G. Diaz, F. Gomes, H.G. Mirchandani, and W.J. Ray, "Microsurgical anatomy of the proximal segments of the middle cerebral artery.," *Journal of neurosurgery*, vol. 61, Sep. 1984, pp. 458-67.
- [8] Y. Hoi, H. Meng, S.H. Woodward, B.R. Bendok, R. a Hanel, L.R. Guterman, and L.N. Hopkins, "Effects of arterial geometry on aneurysm growth: three-dimensional computational fluid dynamics study.," *Journal of neurosurgery*, vol. 101, Oct. 2004, pp. 676-81.
- [9] A.C. Bursleson, C.M. Strother, and V.T. Turitto, "Computer modeling of intracranial saccular and lateral aneurysms for the study of their hemodynamics," *Neurosurgery*, vol. 37, 1995, pp. 774.
- [10] H. Zakaria, A.M. Robertson, and C.W. Kerber, "A parametric model for studies of flow in arterial bifurcations.," *Annals of biomedical engineering*, vol. 36, Sep. 2008, pp. 1515-30.
- [11] A. R .Mantha, G. Benndorf, A. Hernandez, and R. W Metcalfe, "Stability of pulsatile blood flow at the ostium of cerebral aneurysms.," *Journal of biomechanics*, vol.42(8), 2009, pp. 1081-7.
- [12] M. Castro and C. Putman, JR, "Computational fluid dynamics modeling of intracranial aneurysms: effects of parent artery segmentation on intra-aneurysmal hemodynamics," *American Journal of*, vol. 27, 2006, pp. 1703-1709.
- [13] D. Katritsis, L. Kaiktsis, A. Chaniotis, J. Pantos, E.P. Efstathopoulos, and V. Marmarelis, "Wall shear stress: theoretical considerations and methods of measurement.," *Progress in cardiovascular diseases*, vol. 49, 2007, pp. 307-29.
- [14] H. Ujiie, Y. Tamano, K. Sasaki, and T. Hori, "Is the aspect ratio a reliable index for predicting the rupture of a saccular aneurysm?," *Neurosurgery*, vol. 48, Mar. 2001, pp. 495-502; discussion 502-3.
- [15] B. Weir, C. Amidei, G. Kongable, J.M. Findlay, N.F. Kassell, J. Kelly, L. Dai, and T.G. Karrison, "The aspect ratio (dome/neck) of ruptured and unruptured aneurysms.," *Journal of neurosurgery*, vol. 99, Sep. 2003, pp. 447-51.
- [16] K. Funamoto, Y. Suzuki, T. Hayase, T. Kosugi, and H. Isoda, "Numerical validation of MR-measurement-integrated simulation of blood flow in a cerebral aneurysm.," *Annals of biomedical engineering*, vol. 37, Jun. 2009, pp. 1105-16.
- [17] J. Cebal, M. Castro, and J. Burgess, "Characterization of cerebral aneurysms for assessing risk of rupture by using patient-specific computational hemodynamics models," *American Journal*, vol. 26, 2005, pp. 2550-2559.
- [18] M. Shojima, M. Oshima, K. Takagi, R. Torii, M. Hayakawa, K. Katada, A. Morita, and T. Kirino, "Magnitude and role of wall shear stress on cerebral aneurysm: computational fluid dynamic study of 20 middle cerebral artery aneurysms.," *Stroke; a journal of cerebral circulation*, vol. 35, Nov. 2004, pp. 2500-5.
- [19] P. Venugopal, D. Valentino, H. Schmitt, J.P. Villablanca, F. Viñuela, and G. Duckwiler, "Sensitivity of patient-specific numerical simulation of cerebral aneurysm hemodynamics to inflow boundary conditions.," *Journal of neurosurgery*, vol. 106, Jun. 2007, pp. 1051-60.